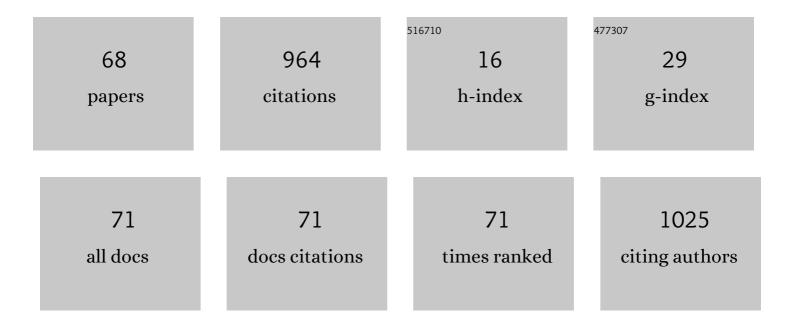
Erick A Juarez-Arellano

List of Publications by Year in descending order

Source: https://exaly.com/author-pdf/9500746/publications.pdf Version: 2024-02-01



#	Article	IF	CITATIONS
1	Novel Rhenium Nitrides. Physical Review Letters, 2010, 105, 085504.	7.8	148
2	Synthesis of Binary Transition Metal Nitrides, Carbides and Borides from the Elements in the Laser-Heated Diamond Anvil Cell and Their Structure-Property Relations. Materials, 2011, 4, 1648-1692.	2.9	100
3	Stability field of the high-(P, T) Re2C phase and properties of an analogous osmium carbide phase. Journal of Alloys and Compounds, 2009, 481, 577-581.	5.5	50
4	In situ observation of the reaction of tantalum with nitrogen in a laser heated diamond anvil cell. Journal of Alloys and Compounds, 2010, 502, 5-12.	5.5	48
5	Reaction of rhenium and carbon at high pressures and temperatures. Zeitschrift Fur Kristallographie - Crystalline Materials, 2008, 223, 492-501.	0.8	40
6	Single-crystal structure of <mml:math <br="" xmlns:mml="http://www.w3.org/1998/Math/MathML">display="inline"><mml:mrow><mml:msub><mml:mrow><mml:mtext>HoBaCo</mml:mtext></mml:mrow><mm ambient conditions, at low temperature, and at high pressure. Physical Review B, 2009, 79, .</mm </mml:msub></mml:mrow></mml:math>	l:m a.2 4 <td>າຫ່ອກາກ></td>	າຫ ່ອກ າກ>
7	Reaction of titanium with carbon in a laser heated diamond anvil cell and reevaluation of a proposed pressure-induced structural phase transition of TiC. Journal of Alloys and Compounds, 2009, 478, 392-397.	5.5	32
8	Single-crystal structure refinement of diaspore at 50 GPa. American Mineralogist, 2007, 92, 1640-1644.	1.9	30
9	High-pressure behavior of the ternary bismuth oxides , and. Journal of Solid State Chemistry, 2009, 182, 767-777.	2.9	30
10	Persistence of the stereochemical activity of the Bi ³⁺ lone electron pair in Bi ₂ Ga ₄ O ₉ up to 50â€GPa and crystal structure of the high-pressure phase. Acta Crystallographica Section B: Structural Science, 2010, 66, 323-337.	1.8	27
11	The crystal structure of InYGe2O7 germanate. Zeitschrift Fur Kristallographie - Crystalline Materials, 2002, 217, 201-204.	0.8	23
12	Immobilization of TiO2 nanoparticles on montmorillonite clay and its effect on the morphology of natural rubber nanocomposites. Polymer Bulletin, 2014, 71, 1295-1313.	3.3	21
13	In situ observation of the reaction of scandium and carbon by neutron diffraction. Journal of Alloys and Compounds, 2011, 509, 1-5.	5.5	20
14	Mechanosynthesis of rhenium carbide at ambient pressure and temperature. International Journal of Refractory Metals and Hard Materials, 2016, 55, 11-15.	3.8	20
15	Planetary ball-mill as a versatile tool to controlled potato starch modification to broaden its industrial applications. Food Research International, 2021, 140, 109870.	6.2	20
16	Synthesis, crystal structure, and preliminary study of luminescent properties of InTbGe2O7. Journal of Solid State Chemistry, 2003, 170, 418-423.	2.9	18
17	Features of formation of channels during laser treatment of AlN ceramics. Optics and Laser Technology, 2010, 42, 172-179.	4.6	18
18	Fabrication of ball-milled MgO–Mg(OH)2-hydromagnesite composites and evaluation as an air-stable hydrogen storage material. International Journal of Hydrogen Energy, 2020, 45, 12949-12960.	7.1	16

#	Article	IF	CITATIONS
19	In situ synchrotron X-ray diffraction study of the formation of TaB2 from the elements in a laser heated diamond anvil cell. Solid State Sciences, 2010, 12, 2059-2064.	3.2	15
20	Formation of scandium carbides and scandium oxycarbide from the elements at high-(P, T) conditions. Journal of Solid State Chemistry, 2010, 183, 975-983.	2.9	15
21	<i>In situ</i> study of the high pressure high-temperature stability field of TaN and of the compressibilities of Ï-TaN and TaON. High Pressure Research, 2013, 33, 633-641.	1.2	15
22	Crystallochemistry of Thortveitite-Like and Thortveitite-Type Compounds. Materials Research Society Symposia Proceedings, 2004, 848, 300.	0.1	14
23	Mechanism to H2 production on rhenium carbide from pyrolysis of coconut shell. International Journal of Hydrogen Energy, 2019, 44, 2784-2796.	7.1	14
24	Microstructural evolution in BaO–Y2O3–Co3O4 mixtures during high-energy milling and its role in the formation of YxBa1â^'xCoO3â^'δand YBaCo4O7. Journal of Alloys and Compounds, 2010, 492, 368-372.	5.5	13
25	Virtual crystal approximation study of nitridosilicates and oxonitridoaluminosilicates. Journal of Physics and Chemistry of Solids, 2008, 69, 1861-1868.	4.0	12
26	Phase transitions in KIO ₃ . Journal of Physics Condensed Matter, 2012, 24, 325401.	1.8	12
27	Coupled Al/Si and O/N order/disorder in BaYb[Si4–xAlxOxN7–x]sialon: neutron powder diffraction and Monte Carlo simulations. Zeitschrift Für Kristallographie, 2007, 222, .	1.1	11
28	In situ observation of self-propagating high temperature syntheses of Ta5Si3, Ti5Si3 and TiB2 by proton and X-ray radiography. Solid State Sciences, 2013, 22, 33-42.	3.2	11
29	Effect of ball to powder ratio on the mechanosynthesis of Re2C and its compressibility. Journal of Alloys and Compounds, 2019, 810, 151867.	5.5	11
30	Defect states and morphological evolution in mechanically processed ZnO + xC nanosystems as studied by EPR and photoluminescence spectroscopy. RSC Advances, 2016, 6, 58709-58722.	3.6	9
31	Chemical stability of superhard rhenium diboride at oxygen and moisture ambient environmental conditions prepared by mechanical milling. Journal of the American Ceramic Society, 2018, 101, 3148-3155.	3.8	9
32	Kinetics of physico-chemical processes during intensive mechanical processing of ZnO–MnO2 powder mixture. Journal of Magnetism and Magnetic Materials, 2011, 323, 2429-2435.	2.3	8
33	Effect of crossâ€linking on the physicochemical, functional and digestibility properties of starch from Macho (<i>Musa paradisiaca</i> L.) and Roatan (<i>Musa sapientum</i> L.) banana varieties. Starch/Staerke, 2016, 68, 584-592.	2.1	8
34	In1.06Ho0.94Ge2O7: a thortveitite-type compound. Acta Crystallographica Section C: Crystal Structure Communications, 2004, 60, i14-i16.	0.4	7
35	Origin and evolution of paramagnetic states in mixtures of ZnO and carbon nanoparticles during intensive mechanical treatment. Journal of Nanoparticle Research, 2015, 17, 1.	1.9	7
36	In1.08Gd0.92Ge2O7: a new member of the thortveitite family. Acta Crystallographica Section C: Crystal Structure Communications, 2002, 58, i135-i137.	0.4	6

#	Article	IF	CITATIONS
37	Compressibility of the nitridosilicate SrYb[Si4N7] and the oxonitridoaluminosilicates MYb[Si4â^'x Al x O x N7âr'x] (x = 2; M = Sr, Ba). Acta Crystallographica Section B: Structural Science, 2006, 62, 424-430.	1.8	6
38	In situ study of the formation of rhenium borides from the elements atÂhigh-(p, T) conditions: Extreme incompressibility of Re7B3 and formation of new phases. Solid State Sciences, 2013, 25, 85-92.	3.2	6
39	High-energy ball milling treatment of soybean for Bacillus thuringiensis culture media. Journal of Bioscience and Bioengineering, 2019, 128, 296-301.	2.2	5
40	Morphological, structural and cytotoxic behavior of starch/silver nanocomposites with synthesized silver nanoparticles using Stevia rebaudiana extracts. Polymer Bulletin, 2021, 78, 1683-1701.	3.3	5
41	altimg="si0032.gif" overflow="scroll" xmlns:xocs="http://www.elsevier.com/xml/xocs/dtd" xmlns:xs="http://www.w3.org/2001/XMLSchema" xmlns:xsi="http://www.w3.org/2001/XMLSchema-instance" xmlns="http://www.elsevier.com/xml/ja/dtd" xmlns:ja="http://www.elsevier.com/xml/ja/dtd" xmlns:mml="http://www.w3.org/1998/Math/MathML"	2.9	4
42	EPR detection of sphalerite ZnO in mechanically treated ZnO+0.1C nanosystem. Materials Science in Semiconductor Processing, 2015, 39, 775-780.	4.0	4
43	Degradation of rhenium carbide obtained by mechanochemical synthesis at oxygen and moisture environmental conditions. Materials Chemistry and Physics, 2019, 229, 15-21.	4.0	4
44	Mechanosynthesis of metastable cubic δ-Ta $1\hat{a}$ `N. Ceramics International, 2020, 46, 23049-23058.	4.8	4
45	Controlled modification of sodium montmorillonite clay by a planetary ball-mill as a versatile tool to tune its properties. Advanced Powder Technology, 2021, 32, 591-599.	4.1	4
46	The layer by layer selective laser synthesis of ruby. Science of Sintering, 2010, 42, 3-13.	1.4	3
47	Melt processing of ethylene–vinyl acetate/banana starch/Cloisite 20A organoclay nanocomposite films: structural, thermal and composting behavior. Iranian Polymer Journal (English Edition), 2020, 29, 723-733.	2.4	3
48	Pt2AuCuNiSn, a new noble metal single-phase high entropy alloy. Journal of Solid State Chemistry, 2021, 294, 121837.	2.9	3
49	Micrometric single crystal germanates obtained using a double-spherical mirror furnace. Crystal Research and Technology, 2004, 39, 833-839.	1.3	2
50	Structural characterization of SmMn2GeO7 single microcrystals by electron microscopy. Acta Crystallographica Section B: Structural Science, 2005, 61, 11-16.	1.8	2
51	Synthesis of TaC and Ta \$\$_2\$\$ 2 C from tantalum and graphite in the laser-heated diamond anvil cell. Science Bulletin, 2014, 59, 5283-5289.	1.7	2
52	Rhenium borides (Re3B and ReB2) mechanosynthesis and their use as a catalyst for H2 production from biomass pyrolysis. Materials Research Bulletin, 2021, 137, 111180.	5.2	2
53	Performance Assessment of Magnesium Anodes Manufactured by Sintering Process. Metals, 2021, 11, 406.	2.3	2
54	Directed laser processing of compacted powder mixtures Al2O3-TiO2-Y2O3. Science of Sintering, 2013, 45, 247-259.	1.4	2

#	Article	IF	CITATIONS
55	Surface modification of carbon steel reinforcement of concrete. Anti-Corrosion Methods and Materials, 2015, 62, 69-76.	1.5	1
56	Synthesis and Characterization of Mg Obtained by Mechanical Alloying and Doped with Al2O3 and Y2O3. Microscopy and Microanalysis, 2017, 23, 584-585.	0.4	1
57	Mechano-Hydrolysis of Non-Conventional Substrates for Biofuel Culture Media. Starch/Staerke, 2019, 71, 1800206.	2.1	1
58	Synthesis and characterization of Pt(Cu0.67Sn0.33). Solid State Sciences, 2020, 105, 106282.	3.2	1
59	Laser Synthesis of Composite Al ₂ O ₃ –Y ₂ Ti _{2Ceramics from Al₂O₃–TiO₂–Y_{2<td>0.3</td><td>1</td>}}	0.3	1
60	Microwave Assisted DNA Hydrolysis for Global Methylation Analysis by Gas Chromatography/Tandem Mass Spectrometry. Journal of the Mexican Chemical Society, 2018, 62, .	0.6	1
61	In1.08Gd0.92Ge2O7: A New Member of the Thortveitite Family ChemInform, 2003, 34, no-no.	0.0	0
62	Transmission Electron Microscopy Study of a New Compound in the System Sm-Mn-Ge-O. Microscopy and Microanalysis, 2003, 9, 868-869.	0.4	0
63	In1.06Ho0.94Ge2O7: A Thortveitite-Type Compound ChemInform, 2004, 35, no.	0.0	0
64	Micrometric Single Crystal Germanates Obtained Using a Double-Spherical Mirror Furnace ChemInform, 2004, 35, no.	0.0	0
65	Incorporation of vanadium(V) into the rutile-type phase of GeO2: the solid solution Ge0.74V0.21â–¡0.05O2. Acta Crystallographica Section E: Structure Reports Online, 2007, 63, i99-i101.	0.2	0
66	Layer-by-layer laser synthesis of composite ceramics in the system Al-Ti-Y-O. Materials Research Society Symposia Proceedings, 2014, 1611, 55-60.	0.1	0
67	Synthesis and Structure–Property Relations of Binary Transition Metal Carbides at Extreme Conditions. NATO Science for Peace and Security Series B: Physics and Biophysics, 2010, , 397-406.	0.3	0
68	Unnamed Pt(Cu0.67Sn0.33) from the Bolshoy Khailyk River, Western Sayans, Russia, and a Review of Related Compounds and Solid Solutions. Minerals (Basel, Switzerland), 2021, 11, 1240.	2.0	0